Angewandte Chemie
Eine Zeitschrift der Gesellschaft Deutscher Chemiker

Supporting Information

Energy Transfer between Spatially Separated Entangled Molecules

*Xiaolan Zhong, Thibault Chervy, Lei Zhang, Anoop Thomas, Jino George, Cyriaque Genet, James A. Hutchison, and Thomas W. Ebbesen**

anie_201703539_sm_miscellaneous_information.pdf

Supporting Information

Table of contents:

1. General methods

Sample fabrication

In this work we used the cyanine dyes TDBC (FEW Chemicals GmbH) (5,6-dichloro-2-[[5,6-dichloro-1-ethyl-3-(4-sulphobutyl)benzimidazol-2-ylidene]propenyl] -1-ethyl-3-(4-sulphobutyl)benzimidazolium hydroxide, $\mathbf{MW}_{TDBC}$=762.53 g/mol) as the donor and another cyanine dye BRK 5714 (Organica Feinchemie GmbH) (1-(3-Sulfopropyl)-2-(2-{[1-(3-sulfopropyl)naphtho[1,2-d]thiazol-2(1H)-ylidene]methyl}-1-butenyl)naphtha[1,2-d]thiazoliumhydroxide, $\mathbf{MW}_{BRK}$=782.067) as the acceptor. Both the donor D and acceptor A molecules undergo self-organization in deionized (DI) water to form J-aggregates with high oscillator strengths and narrow transition line widths, suitable for achieving strong coupling at room temperature. To begin, a 30 nm thick silver film was sputtered on a glass substrate, upon which was spin cast a film of polyvinyl alcohol (PVA) in which TDBC was dispersed. This was followed by a spacer layer consisting of poly(methyl methacrylate) (PMMA) on which a layer of PVA with BRK was spin cast. The whole thickness of dielectric layers was fixed at ~330 nm and the thickness of the TDBC and BRK layers were the same but adjusted to accommodate the spacer thickness, i.e. $t_D = t_A = (330\text{ nm} - h)/2$. The DI water solutions for spin coating contained 0.5% TDBC and 3% PVA by weight, and 0.5% BRK and 3% PVA by weight respectively. Finally, a 30 nm thick silver film was sputtered upon the spin cast film.

2. Transmission and reflection spectra of donor-acceptor strongly coupled cavities

The normalized transmission and reflection spectra of the D-A strongly coupled cavity are shown in Figure S1a and S1b with various spacer thicknesses ranging from 10 nm to 75 nm and

compared those of a cavity strongly coupled only to D.

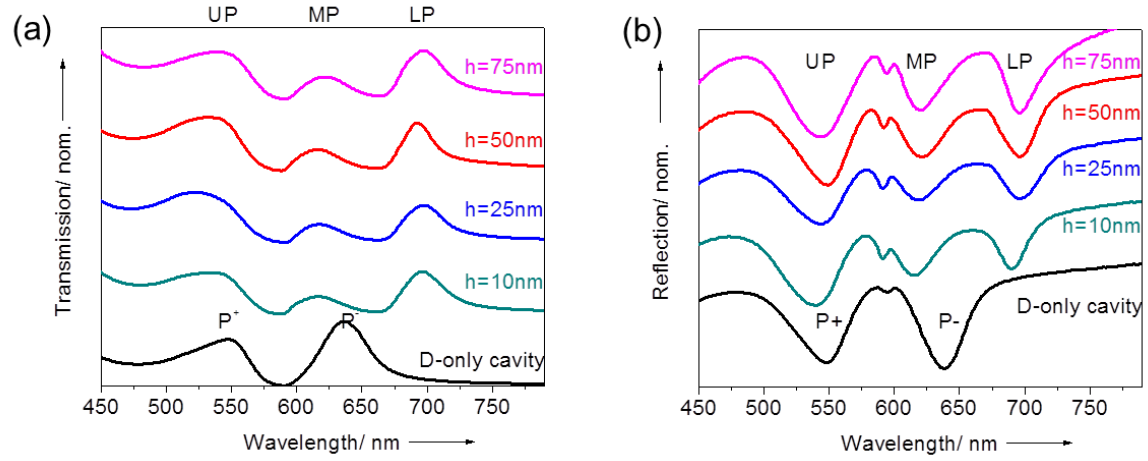

Figure S1. Normalized transmission (a) and reflection (b) spectra from varying spacer thicknesses between D (TDBC) and A (BRK) in the strongly coupled cavity.

3. Three oscillator coupled model

The Hamiltonian for 3 oscillator coupled system can be expressed as:

$$\begin{pmatrix} E_\gamma(\theta) & \hbar\Omega_D/2 & \hbar\Omega_A/2 \\ \hbar\Omega_D/2 & E_{exD} & 0 \\ \hbar\Omega_A/2 & 0 & E_{exA} \end{pmatrix} \begin{pmatrix} \alpha_\gamma \\ \alpha_{exD} \\ \alpha_{exA} \end{pmatrix} = E_{pol}(\theta) \begin{pmatrix} \alpha_\gamma \\ \alpha_{exD} \\ \alpha_{exA} \end{pmatrix} \qquad \text{(S1)}$$

where $\mathrm{E_\gamma(\theta) = E_0(1\text{-}\sin^2(\theta)/n^2)^{-1/2}}$ is the cavity mode energy, E_0 is the cavity cutoff energy and *n* is the cavity effective refractive index. E_{exD} and E_{exA} are the energies of the two exciton species and $E_{pol}(\theta)$ is the polariton energy. $\hbar\Omega_D$ and $\hbar\Omega_A$ are the light-matter coupling energies. There are three unique solutions for $E_{pol}(\theta)$ and thus the polariton energy dispersion comprises the three branches UP, MP and LP. The "zero" term in this equation means there is no interaction between donor and acceptor outside cavity.

4. Dispersion spectra of donor and donor-acceptor strongly coupled cavities

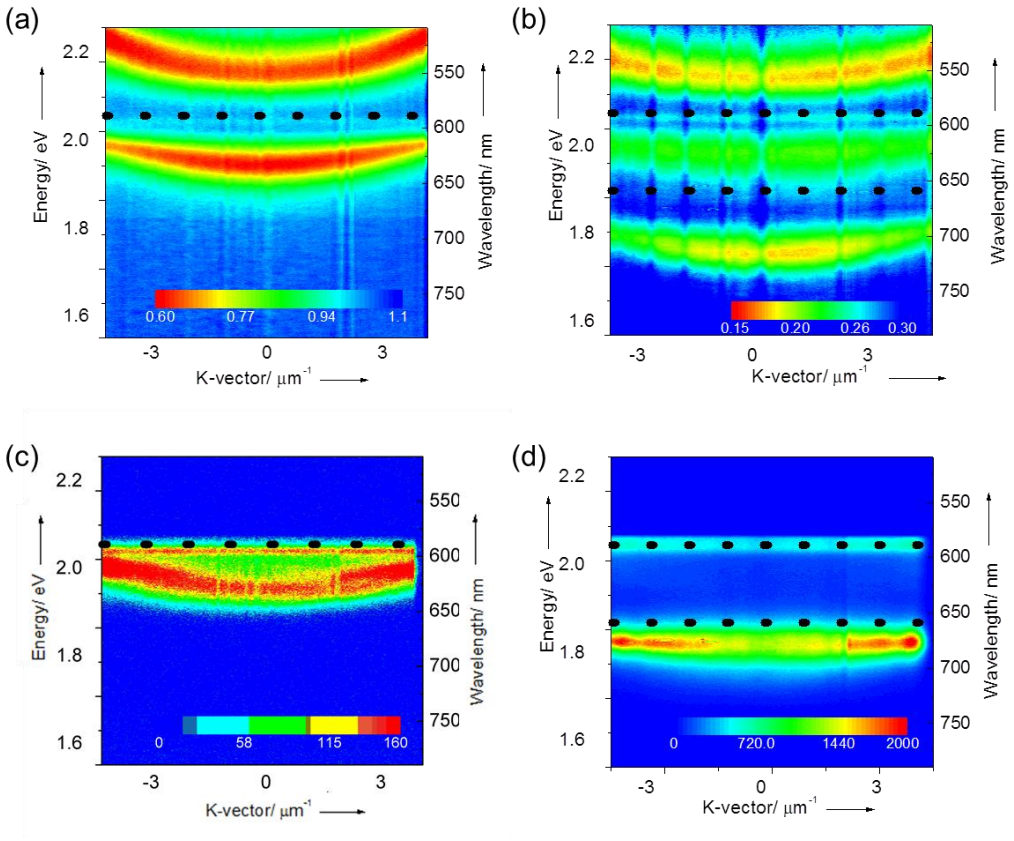

Figure S2. (a) Examples of the reflection dispersion plots of the D (TDBC) strongly coupled cavity. (b) Examples of the reflection dispersion plots for the D-A (with 50 nm PMMA spacer) strongly coupled cavity. The black dotted lines indicate the position of the non-dispersive exciton energies (TDBC and BRK). (c) Examples of the emission dispersion plots for D (TDBC) strongly coupled cavity excited at 530 nm. (d) Examples of the emission dispersion plots for the D-A (with 50 nm PMMA) strongly coupled cavity excited at 530 nm. The black dotted lines indicate the position of the non-dispersive exciton energies.

5. The steady state and time resolved measurement methods

Steady-State Spectroscopy

Steady-state transmission and reflection spectra were taken on a Shimadzu UV3101 spectrometer. Steady-state fluorescence spectra were taken with a Horiba Jobin Yvon-Spex Fluorolog-3 fluorimeter.

Time-Resolved Measurements

Narrow band (line width = 6 nm), 150 fs pulses (SpectraPhysics laser) centered at 530 nm were used for the transient spectroscopy. The spectrum was recorded using low-energy pump pulses to avoid spurious effects and exciton−exciton annihilation in the TDBC and BRK J-aggregates. The differential transmittance spectra were recorded at different time delays after the excitation pulse. The kinetic traces were then obtained by plotting the differential transmittance at a given wavelength as a function of time. The kinetic analysis to extract the lifetimes was carried out using the following method.

The excited-state population of the system after excitation of the donor with a δ-pulse can be described by the following set of equations:

$$\begin{cases} \dfrac{dD(t)}{dt} = -(k_d + k_t)D(t) \\ \dfrac{dA(t)}{dt} = D(t)k_t - A(t)k_a \end{cases} \tag{S2}$$

Where D(t) is the concentration of the donor molecules in the excited state, A(t) is the concentration of excited acceptor molecules, k_d is the rate constant of donor-molecule de-excitation in the absence of the acceptor and it is equal to $(k_r + k_{nr})$, and k_a is the acceptor de-excitation rate constant and k_t is the rate constant of resonance energy transfer. Solving Equation (S2) results in the following functions describing the decay of exited-state concentrations of the donor and acceptor as

$$\begin{aligned} D(t) &= D_0 e^{-(k_d + k_t)t} \\ A(t) &= \frac{-D_0 k_t}{k_d + k_t - k_a} e^{-(k_d + k_t)t} + \frac{D_0 k_t}{k_d + k_t - k_a} e^{-k_a t} \end{aligned} \tag{S3}$$

where D_0 is the excited-state population of the donor at t = 0. The negative term in the expression of $A(t)$ reflects a rise component due to energy transfer from donor to acceptor with rate constant $(k_d + k_t)$.[1]

Transient spectra, decay kinetics and static spectra

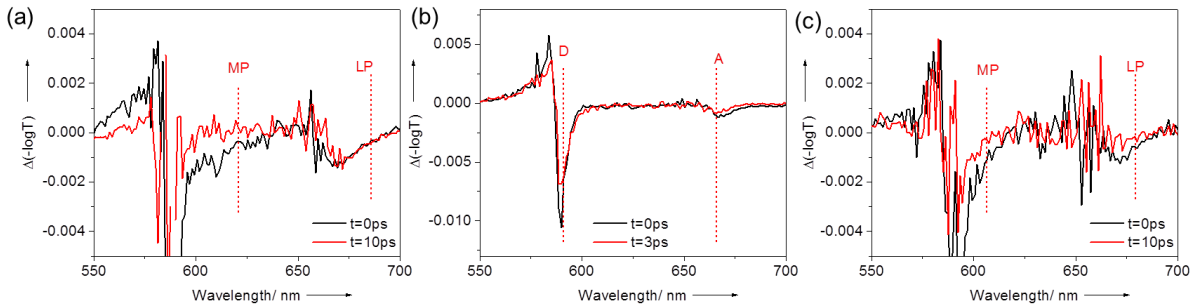

Figure S3. (a) Transient absorption spectra of D-A strongly coupled system at different decay times; (b) Transient absorption spectra of D-A layers on top of a 30 nm Ag film at different decay times (no cavity); (c) Transient absorption spectra of donor-acceptor in the detuned cavity at different decay times.

Figure S3a shows the transient spectra for a strong coupled D-A system. The spectra are identical in the absence of strong coupling, e.g. when the second mirror is missing (Figure S3b), i.e. no cavity, or the cavity is detuned (Figure S3c). The decay kinetics are shown in Figure S4 as explained in the figure legend.

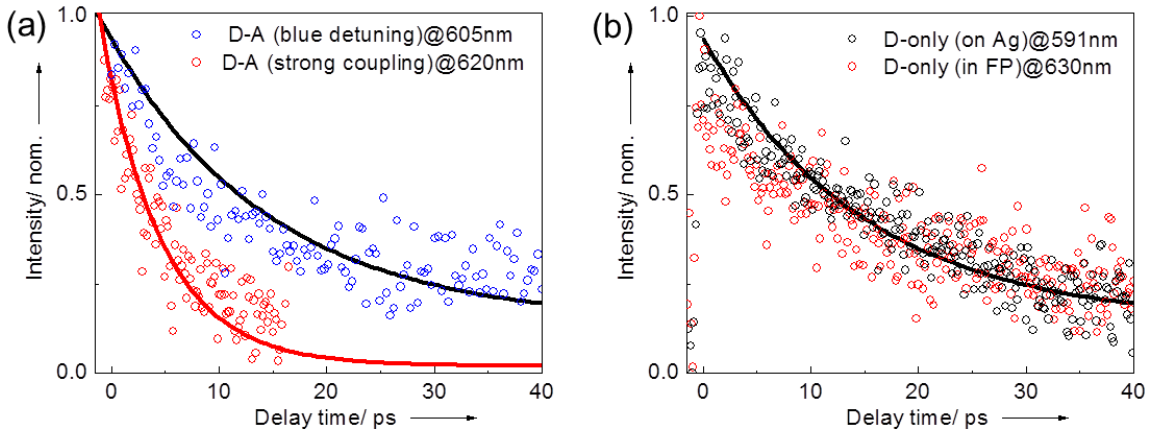

Figure S4. (a) The decay kinetics of the D-A with a 50 nm spacer layer measured at 605 nm for a cavity blue-detuned to 560 nm (blue circles). It is compared to a strongly coupled system in resonance at 590nm, already shown in Figure 4 (red circles). The black and red lines are the fits to the data. (b) The decay kinetics of the D–only outside cavity at the TDBC absorption

maximum 591 nm (black circles), and of P^- in the strongly coupled system at 630 nm (red circles). The solid black line is a fit to the data.

Effect of D and A concentration on energy transfer efficiency:

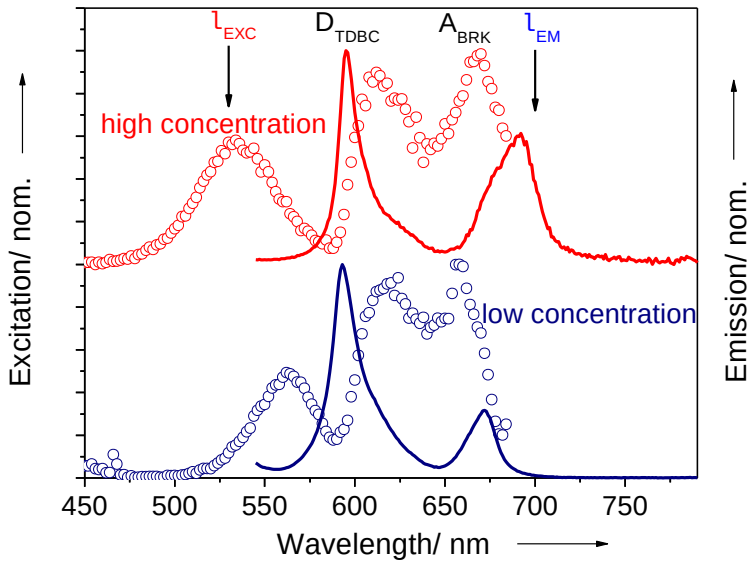

Figure S5: Normalized excitation (dots) and emission (solid line) spectra for h=50nm and for two concentrations (high: 1:6 j-aggregate to PVA weight ratio, and low: 1:15). Both are in the strongly coupled regime but at the lower concentration the coupling strength is much lower and the energy transfer decreases relative to D emission.

6. Cavity Förster energy transfer between spatially separated entangled molecules

In order to place our energy transfer results in the context of Förster theory, we model below the elementary energy transfer process between a donor molecule (D) initially in its excited state, and an assembly of acceptor molecules (A) initially in their ground-states, mediated by the resonant optical mode of the cavity. The D and A molecules are distributed at either side of a Fabry-Pérot cavity having its 2nd optical mode resonantly tuned to the D absorption peak, and are spatially separated by a dielectric spacer of variable thickness *h* as shown in Figure S6a.

Using the multipolar method [2] we can write the probability amplitude of a coherent excitation transfer between D and A as:

$$M = \langle g_D, e_A | H_{int} | e_D, g_A \rangle \tag{S4}$$

where $g(e)_{D(A)}$ denotes the ground-state (excited-state) of the donor (acceptor) molecule. The dipole-dipole interaction Hamiltonian H_{int} couples the D and A transition dipole operators $\hat{d}_{D(A)}$ via the cavity electric field operator $E(z)$ [2], and is given by:

$$H_{int} = -\hat{d}_D \cdot \hat{E}(z_D) - \hat{d}_A \cdot \hat{E}(z_A) \tag{S5}$$

where $z_{D(A)}$ is the position of the D (A) molecule along the optical axis z. At second order in H_{int}, M reads:

$$M = \sum_I \frac{\langle f | H_{int} | I \rangle \langle I | H_{int} | i \rangle}{E_i - E_I} \tag{S6}$$

where the initial states $|i\rangle = |e_D, g_A, 0_c\rangle$ of energy E_i and final states $|f\rangle = |g_D, e_A, 0_c\rangle$ are linked by all the possible intermediate states $|I\rangle$ of energy E_I. In the above notation, $|0(1)_c\rangle$ indicates the number of photons occupying the cavity mode of energy $E_c = \hbar\omega_c$, momentum $\vec{k}_c$ and polarization $\vec{\epsilon}_C$. The key point of our model is to impose in the summation over all states $|I\rangle$ that they respect the cavity dispersion relation $\omega_c(\vec{k}_c)$. In particular, this single mode restriction suppresses the near field D-A energy transfer, as it should be the case due the presence of the spacer. The two possible intermediate states for the energy transfer process are those represented in Figure 1c of the main text, and correspond to the rotating and counter-rotating terms of the strong coupling regime. [3] Upon summation over those intermediate states, we obtain expression (1) of the main text, which does not depend on the absolute separation distance between D and A, but only on their coupling strengths to the dressing cavity field. Applying the Fermi golden rule to one initially excited D and N initially at rest A, we obtain the energy transfer rate:

$$\Gamma(h) = \frac{2\pi}{\hbar} \rho \sum_{h/2 < z_A < L/2} |M(z_A)|^2 \tag{S7}$$

where ρ is the density of acceptor states. In the language of strong coupling, this energy transfer process is achieved by two Rabi oscillations as sketched in Figure S6b. As the spacer thickness h increases, less and less molecules participate in the energy transfer process, while the Rabi splitting decreases concomitantly (see Figure S6c). We show in Figure S6d that indeed, the energy transfer rate $\Gamma(h)$ drops as the square of the Rabi frequency Ω_R, confirming this intuitive picture. A striking implication of this result is that, as long as one maintains the same coupling strength, the energy transfer process remains distance-independent.

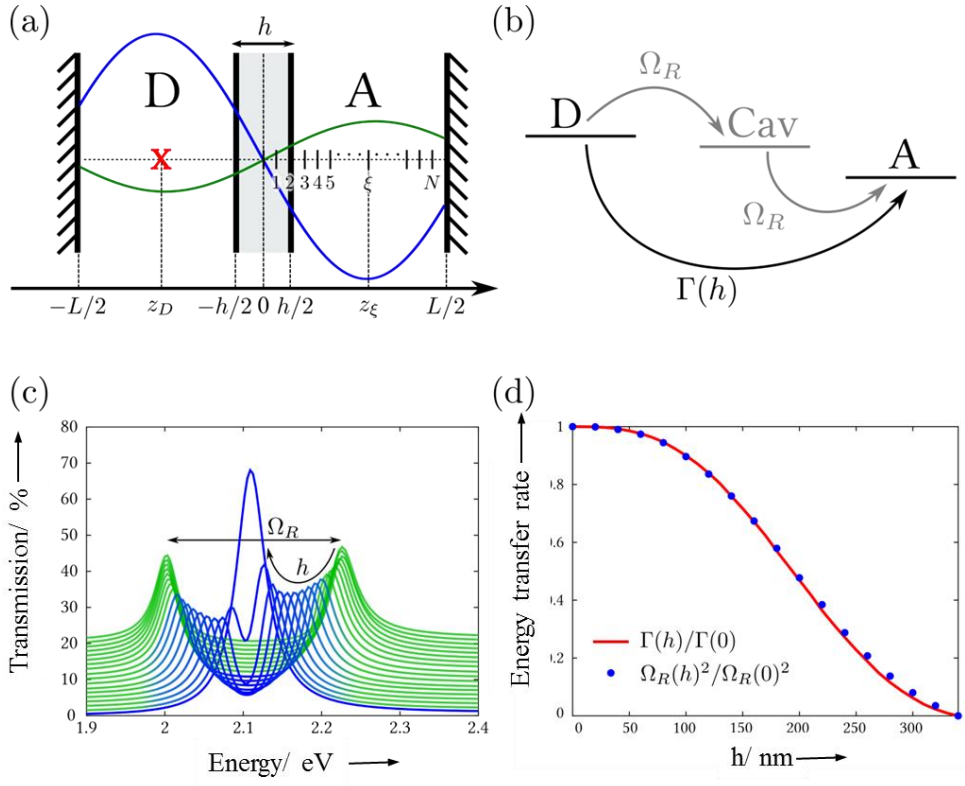

Figure S6. (a) Schematic representation of the 2nd mode cavity of length *L* embedding the donor (D) and acceptor (A) molecules, separated by a dielectric spacer of thickness h. The initially excited D at position z_D can transfer its energy to any A molecule at position z_ξ. The blue (green) curve represents the real (imaginary) part of the electric field in the cavity as computed by transfer matrix method. (b) Sketch of the energy transfer process involving two Rabi oscillations. (c) Calculated transmission spectrum of the cavity embedding the D and A molecules for different spacer thicknesses h. (d) Energy transfer rate $\Gamma(h)$ as a function of

spacer thickness, normalized to the energy transfer rate without spacer. The blue dots represent the normalized Rabi splitting squared, as extracted from panel (c).

[1] S. P. Laptenok, J. W. Borst, K. M. Mullen, I. H. M. van Stokkum, A. J. W. G. Visser and H. van Amerongen, Phys. Chem. Chem. Phys. **2010**, 12, 7593-7602.

[2] D. P. Craig, T. Thirunamachandran, Molecular Quantum Electrodynamics, Academic Press Inc. (London) Ltd. Academic Press, **1984**.

[3] J. J. Hopfield, Phys. Rev. **1958**, 112, 1555.